Chemical Science

Accepted Manuscript

Chemical Science

rsc.li/chemical-science

Volume 9
Number 1
7 January 2018
Pages 1-268

ISSN 2041-6539

ROYAL SOCIETY OF CHEMISTRY

EDGE ARTICLE
Xinjing Tang et al.
Caged circular siRNAs for photomodulation of gene expression in cells and mice

This is an Accepted Manuscript, which has been through the Royal Society of Chemistry peer review process and has been accepted for publication.

Accepted Manuscripts are published online shortly after acceptance, before technical editing, formatting and proof reading. Using this free service, authors can make their results available to the community, in citable form, before we publish the edited article. We will replace this Accepted Manuscript with the edited and formatted Advance Article as soon as it is available.

You can find more information about Accepted Manuscripts in the Information for Authors.

Please note that technical editing may introduce minor changes to the text and/or graphics, which may alter content. The journal's standard Terms & Conditions and the Ethical guidelines still apply. In no event shall the Royal Society of Chemistry be held responsible for any errors or omissions in this Accepted Manuscript or any consequences arising from the use of any information it contains.

ROYAL SOCIETY OF CHEMISTRY

rsc.li/chemical-science

Cu-Catalyzed Enantioconvergent Deborylative Alkynylation

Joshua F. Head, Tanner J. Schubert, Biyu Zhao, Yuyang Dong*[a]
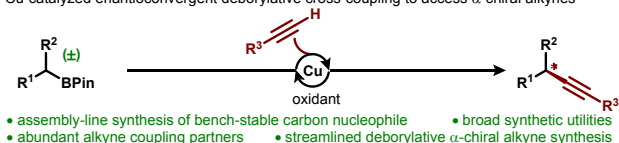
Alkylboronic pinacol esters represent a highly attractive class of reagents due to their modular synthesis and unique reactivity conferred by the vacant boron p-orbital. However, their direct application in asymmetric C–C cross-coupling reactions remains underexplored. Herein, we report a Cu-catalyzed deborylative strategy to access α-chiral alkynes that delivers good enantioselectivity and accommodates a broad range of functional groups and heterocycles. The reaction is proposed to proceed through a radical-relay pathway: an aminyl radical-mediated C–B bond cleavage followed by Cu-catalyzed asymmetric alkynylation. The reaction mechanism was probed using a combination of radical clock ring-opening study, radical trapping experiments, and enantioconvergence test with enantioenriched starting materials. Density functional theory (DFT) calculations demonstrate the feasibility of a Cu-mediated inner-sphere C–C bond-forming pathway and attribute the observed enantioselectivity to attractive ligand-substrate halogen-π interactions.
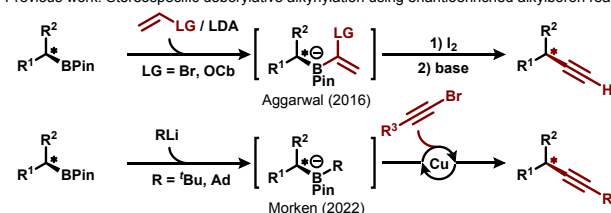
Introduction

Alkylboronic pinacol esters have emerged as highly versatile reagents in organic synthesis.[1-5] Their capacity for iterative homologation through 1,2-boronate rearrangement allows for efficient and stereocontrolled assembly of complex frameworks.[6-9] The unique stability and reactivity of α-borylcarbanions render them readily accessible intermediates for alkyl skeleton construction.[10-15] Despite their synthetic potentials imparted by the vacant boron p orbital, the application of alkylboronic pinacol esters in asymmetric deborylative C–C cross-coupling remains limited due to sluggish transmetalation and competing protodeboronation pathways.[16] In particular, an enantioconvergent deborylative alkynylation protocol could unlock powerful synthetic disconnections by combining the modularity of alkylboronic pinacol esters and versatility of alkynyl groups (Figure 1A)—yet such a transformation remains elusive. Seminal work by Aggarwal[17] and Morken[18] (Figure 1B) demonstrated the potential of enantioenriched alkylboronic pinacol esters for α-chiral alkyne synthesis via (1) enantiospecific Zweifel-type alkenylations followed by 1,2-elimination, and (2) stereoretentive transmetalation to CuCN facilitated by alkyl lithium reagents and subsequent coupling with alkynyl bromides, respectively. We reasoned that an alternative enantioconvergent strategy, which directly engages racemic alkylboronic pinacol esters with readily available terminal alkynes, could provide a streamlined approach to these valuable products. We herein disclose the first enantioconvergent deborylative alkynylation protocol facilitated by ligand design and proceeding through a Cu-catalyzed radical relay.[19-21]
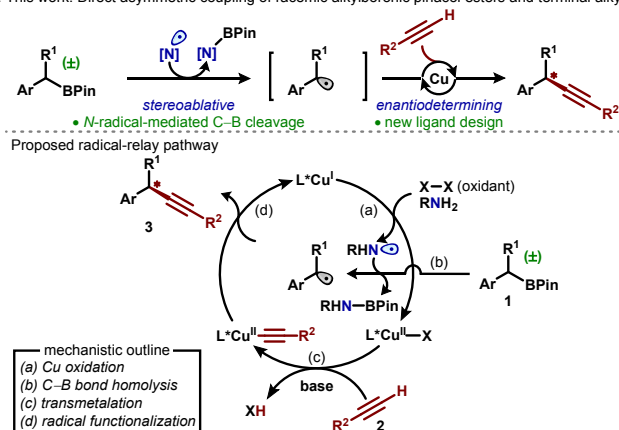

Figure 1. (A) A Cu-catalyzed asymmetric deborylative cross-coupling approach to α-chiral alkyne synthesis; (B) Stereospecific transformations as the only examples of deborylative protocols to access α-chiral alkynes; (C) Employing alkylboronic pinacol esters in enantioconvergent alkynylation through single-electron processes.

We envisioned that this transformation could be achieved through two key mechanistic steps (Figure 1C): (1) the homolytic cleavage of C–B bonds and (2) the asymmetric functionalization of alkyl radicals via Cu(II) alkynyl intermediates.[22-31] The single-electron activation of alkylboronic pinacol esters is often hindered by their high oxidation potential.[32-34] We previously overcame this challenge by employing an in situ generated aminyl radical to promote C–B bond homolysis through an inner-sphere pathway.[34-36] Following the C–B bond activation (steps a-b), we propose that the resulting prochiral radical engages an in situ generated homocoupling of terminal alkynes and (2) undesired C–N coupling with amine activator. We further reasoned that these

[a.] Department of Chemistry, Colorado State University, Fort Collins, Colorado 80523, United States E-mail: Yuyang.Dong@colostate.edu

ARTICLE

challenges could be circumvented through the judicious choice of base additives and oxidants to balance the relative rates among alkyne transmetalation, C–B bond activation, and radical functionalization steps. We herein report the successful implementation of this strategy for an enantioconvergent deborylative alkynylation protocol and the corresponding mechanistic studies to guide our future expansion of this C–C cross-coupling platform.

Results and discussion

Reaction optimization

We initiated our investigation by examining the cross-coupling between alkylboronic pinacol ester **1a** and 2-ethynylthiophene **2a**. We tested a range of copper sources, chemical oxidants, amine additives, external bases, and reaction solvents (See Supporting Information, Table S1 for full optimization details). The focus on inda(box)-type ligands (box: bisoxazoline) was motivated by the pioneering work of Liu et al.,[20-23] who demonstrated their utility in asymmetric radical alkynylation. A combination of cuprous trifluoromethanesulfonate benzene complex and parent inda(box) ligand **L1** yielded product **3a** with moderate yield and enantioselectivity (Table 1). We identified two potential strategies to improve the reaction selectivity: (1) tuning the ligand bite-angle via *meso*-substitution[37] and (2) enhancing ligand-substrate interactions by installing distal substituents.[38-40] While introducing methyl (**L2–L3**) or other groups (Table S1) to the *meso*-position diminished the reaction yield,[41] modifications at the phenyl *meta*-position (**L4–L6**) proved beneficial. In particular, bromine substitution in **L6** delivered the highest yield and enantioselectivity. We attributed this observation to ligand-substrate halogen-π interactions[40, 42, 43] within the C–C bond-forming transition structures as indicated by DFT calculations (*vide infra*).

Among the oxidants tested, feedstock chemical di-*tert*-butyl peroxide (ᵗBuO)₂ provided the highest yield of **3a** while minimizing alkyne homocoupling compared to other oxidants commonly employed in cross-coupling reactions (entries 4–6, see also Table S2).[19-21] We anticipate that the amine additive is crucial in facilitating the single-electron activation of alkylboron reagents.[34-36] A range of substituted anilines and alkylamines were tested, with the highest yield and enantioselectivity obtained using a stoichiometric amount of aniline (entries 9–12, see also Table S2). No C–N coupling was observed under the optimized reaction conditions. Reaction carried out in toluene (entries 7–8, Table S2) at 60 °C (entries 13–14) yielded the optimal result. An exogenous base was employed to promote the alkyne transmetalation step, with the best outcome achieved using Cs₂CO₃ (Table S2).

Table 1. Reaction Optimisation[a]

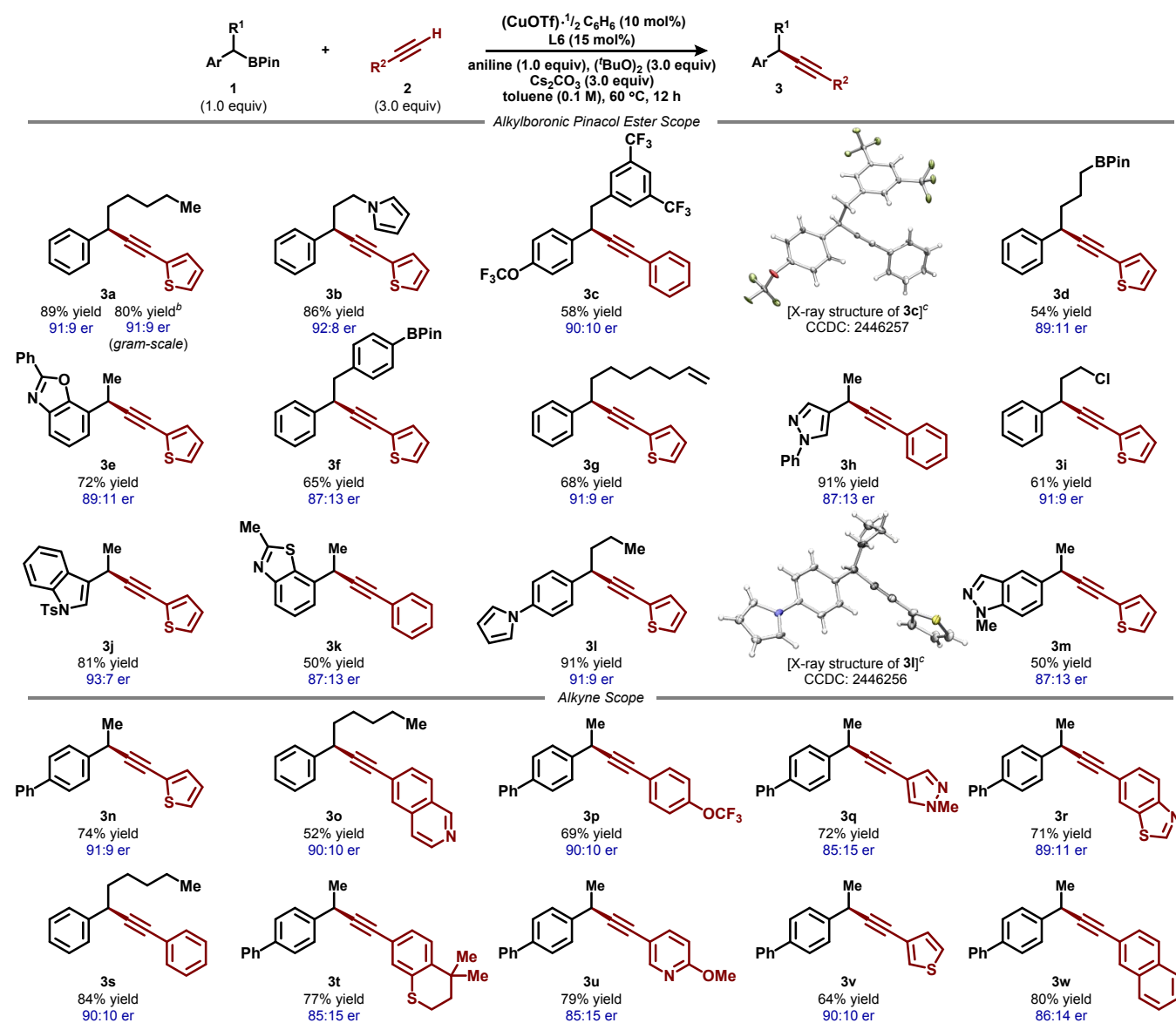| entry	variation from standard conditions	yield (%)	er
1	none	83	91:9
2	CuI as copper source	46	90:10
3	Cu(CH₃CN)₄PF₆ as copper source	44	88:12
4	(cumylO)₂ as oxidant	38	90:10
5	PhI(OAc)₂ as oxidant	0	-
6	ᵗBuOOH as oxidant	0	-
7	DCM as solvent	56	88:12
8	PhCl as solvent	66	89:11
9	DMAP as additive	<5	-
10	4-trifluoromethylaniline as additive	<5	-
11	4-methoxyaniline as additive	70	90:10
12	no additive	0	-
13	23 °C	12	91:9
14	80 °C	58	89:11

Ligand Optimization:
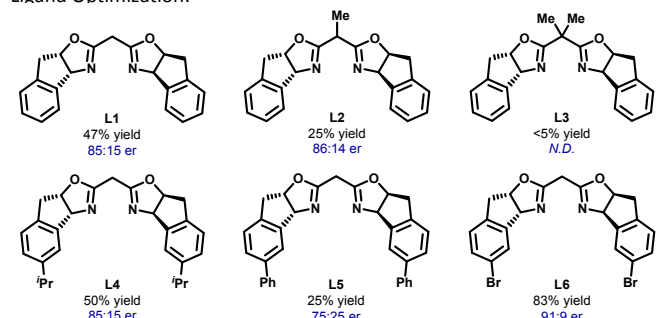
[a]Reaction conditions unless otherwise noted: 4,4,5,5-tetramethyl-2-(1-phenylhexyl)-1,3,2-dioxaborolane (**1a**, 0.10 mmol), 2-ethynylthiophene (**2a**, 0.30 mmol), aniline (0.10 mmol), specified catalyst mixture, di-*tert*-butyl peroxide (0.30 mmol), and toluene (0.1 M); reaction yields were determined by ¹H NMR spectroscopy of the crude reaction mixture using 1,1,2,2-tetrachloroethane as an internal standard (see the Supporting Information for details). The enantiomeric ratio (er) of product **3a** was determined by chiral high-performance liquid chromatography (HPLC) analysis.

Substrate scope

With the optimized reaction conditions, we assessed the functional group tolerance and scope of compatible alkylboronic pinacol esters and alkynes (Figure 2). The absolute configuration of the major enantiomer was determined by a combination of optical rotation measurements and the solid-state structures of products **3c** and **3l**. The reaction proceeds effectively in the presence of various heterocycles commonly found in pharmaceuticals,[44-47] including thiophene (**3a**), pyrrole (**3b**, **3l**), benzoxazole (**3e**), pyrazole (**3h**), indole (**3j**), benzothiazole (**3k**, **3r**), indazole (**3m**), isoquinoline (**3o**), thiochromane (**3t**), and pyridine (**3u**).

Functionalization of substrates containing aza-heterocycles (**3h**, **3m**, **3o**, **3q**, **3r**) proceeds effectively with no detectable side products resulting from radical addition. Functional groups prone to oxidation, such as thioether (**3t**), are tolerated under reaction conditions. The protocol is compatible with weak allylic (**3g**)/benzylic C–H bonds (**3c**, **3f**) and proceeds smoothly in the

Figure 2. Reaction Scope[a]

Reaction conditions: 1 (1.0 equiv) + 2 (3.0 equiv), (CuOTf)·$\frac{1}{2}$ C$_6$H$_6$ (10 mol%), L6 (15 mol%), aniline (1.0 equiv), (^{t}BuO)$_2$ (3.0 equiv), Cs$_2$CO$_3$ (3.0 equiv), toluene (0.1 M), 60 °C, 12 h → 3

Alkylboronic Pinacol Ester Scope

3a 89% yield / 80% yield[b] 91:9 er / 91:9 er (gram-scale)
3b 86% yield 92:8 er
3c 58% yield 90:10 er
[X-ray structure of **3c**][c] CCDC: 2446257
3d 54% yield 89:11 er
3e 72% yield 89:11 er
3f 65% yield 87:13 er
3g 68% yield 91:9 er
3h 91% yield 87:13 er
3i 61% yield 91:9 er
3j 81% yield 93:7 er
3k 50% yield 87:13 er
3l 91% yield 91:9 er
[X-ray structure of **3l**][c] CCDC: 2446256
3m 50% yield 87:13 er

Alkyne Scope

3n 74% yield 91:9 er
3o 52% yield 90:10 er
3p 69% yield 90:10 er
3q 72% yield 85:15 er
3r 71% yield 89:11 er
3s 84% yield 90:10 er
3t 77% yield 85:15 er
3u 79% yield 85:15 er
3v 64% yield 90:10 er
3w 80% yield 86:14 er

[a]All yields were obtained using 0.50 mmol of alkylboronic pinacol ester substrates unless otherwise noted. Enantiomeric ratio (er) was determined by chiral HPLC analysis. [b]Reaction carried out on a 5.00 mmol scale of substrate **1a**. [c]Solid-state molecular structure of **3c** and **3l** with thermal ellipsoids at 50% probability level. Colour scheme: S, yellow; N, blue; C, grey, O, red, F, yellow-green, H, white.

presence of alkyl halide (**3i**). These results highlight the orthogonality of the deborylative alkynylation approach to emerging catalytic strategies, such as asymmetric C–H functionalization or Sonogashira-type transformations.[22-30] The protocol exhibits high selectivity between different alkylboronic pinacol esters. For substrates containing additional aryl (**3f**) or primary alkyl boronic esters (**3d**), only the products resulting from benzylic functionalization were obtained. To further highlight the synthetic utility of the enantioconvergent alkynylation protocol, the synthesis of **3a** was carried out on a 5.0 mmol scale, resulting in comparable yield and enantioselectivity to the 0.5 mmol scale reactions.

Mechanistic investigation

Building on the successful application of the alkynylation protocol across a broad substrate scope, we integrated experimental and theoretical studies to elucidate the reaction mechanism and origin of enantioselectivity, with the goal of guiding future chiral ligand design and advancing the asymmetric deborylative C–C cross-coupling platform. Alkynylation of radical clock substrate **4** led to the formation of product **5a** and ring-opened **5b**, indicating the intermediacy of an alkyl radical (Figure 3A). Radical trapping experiments were carried out using TEMPO and CBrCl$_3$ (Figure 3B). In both cases, the formation of **3n** was inhibited while the TEMPO-coupled product **6** and brominated product **7** were observed in 32% and 26% yield, respectively, supporting the involvement of an alkyl radical intermediate. Subjecting enantiomerically enriched *R*- or *S*-**1n** to the reaction conditions resulted in the generation of

product **3n** with a similar enantiomeric ratio favoring the same major enantiomer, indicating the loss of stereochemical information prior to C–C bond formation (Figure 3C).
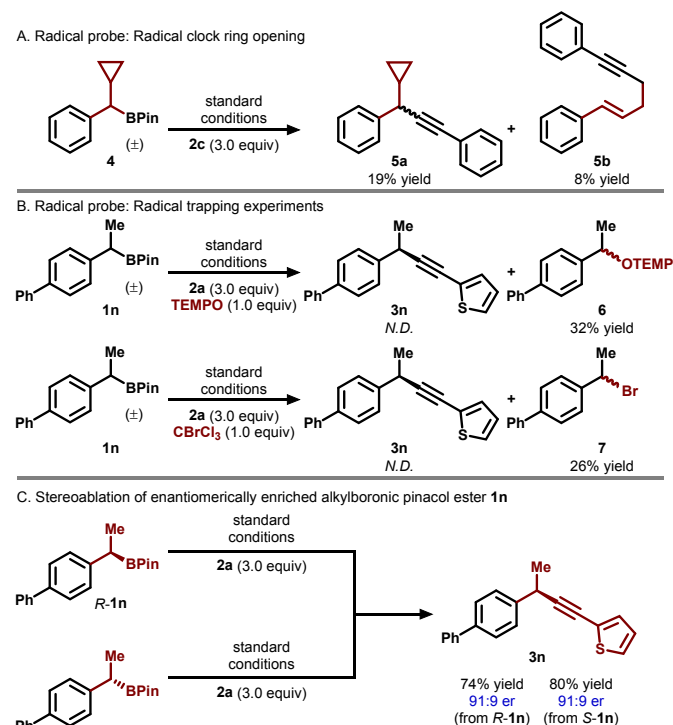

Figure 3. Mechanistic probes for the asymmetric deborylative alkynylation (Reactions were carried out on a 0.10 mmol scale. Yields were determined by ^{1}H NMR spectroscopy of the crude product mixture using 1,1,2,2-tetrachloroethane as an internal standard.) (A) The proposed alkyl radical formation is supported by radical ring opening of the cyclopropyl substituent in substrate **4**. (B) The alkyl radical intermediates can be intercepted using radical traps. (C) Stereochemical information is lost after the generation of an alkyl radical.

Computational studies were next carried out to investigate our proposed mechanism and elucidate the origins of enantioconvergence. Dispersion-corrected DFT calculations were performed at the B3LYP-D3(BJ)/def2-TZVP-SMD(toluene)//B3LYP-D3(BJ)/def2-SVP & def2-TZVP(Cu, Br)-SMD(toluene) level of theory.[48-54] We modelled the coupling between alkylboronic pinacol ester **1n** and 2-ethynylthiophene **2a** with ligand **L6** via an inner-sphere pathway.[22] Our previous computational study[35] indicated that among several plausible C–B bond activation pathways, inner-sphere aminyl radical activation is kinetically most favourable. We propose that an analogous mechanistic framework underlies the alkynylation system. Control experiments (Table 1, entries 10-12) underscore the critical role of aniline in this protocol. We hypothesized that substrate **1n** undergoes aminyl-radical-mediated C–B bond cleavage: H-atom transfer between aniline and *tert*-butoxy radical generates the anilinyl radical (Figure 1C), which in turn initiates C–B bond homolysis in **1n** to produce alkyl radical **9**·and ArNH–Bpin as a stoichiometric byproduct. (see SI, Scheme S1-2 for details).[35] Computational results (Figure 4A) indicated that the addition of radical **9** to divalent Cu intermediates **8**[55] is slightly endergonic, generating formal Cu(III) intermediates **10$_R$** (ΔG = 1.7 kcal/mol) and **10$_S$** (ΔG = 1.5

kcal/mol). The subsequent C–C bond formation proceeds via competing diastereomeric reductive elimination transition structures (TSs) **TS1$_R$** and **TS1$_S$**, with retention of configurations at the benzylic positions. While formation of **10$_s$** is slightly favoured thermodynamically (ΔΔG = 0.2 kcal/mol), the R-enantiomer pathway is kinetically preferred (ΔΔG‡ = 0.7 kcal/mol, consistent with experimental observations), indicating that radical **9** capture is likely reversible and proceeds with a low barrier. Analysing the noncovalent interaction (NCI) isosurfaces of **TS1$_R$** and **TS1$_S$** attributes the selectivity to attractive ligand-substrate halogen-π interactions[40, 42, 43] between a bromine substituent and an axial 2-thiopheneacetylide ligand (Figure 4B). The bond metrics (Br–Ar(centroid) distance: 3.61 Å; C–Br–Ar(centroid) angle: 104.4°)[56] are consistent with halogen–π interactions observed in enzymatic systems, where aromatic side chains align to facilitate arene electron density donation to the σ-hole of the C–Br bond.[42, 57] Similar interaction is absent in **TS1$_S$** due to the opposing orientation of ligand Br substituent and the alkynyl group (Scheme S7).[58]

A. Computed Gibbs energy profile of C–C bond formation via an inner-sphere mechanism
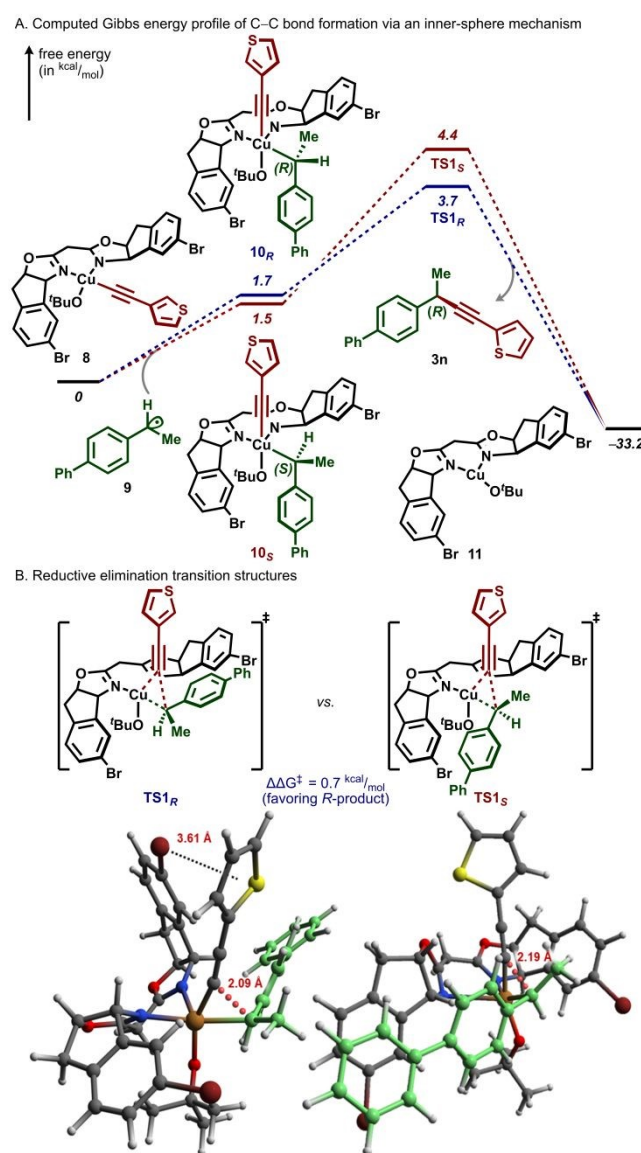
B. Reductive elimination transition structures

Figure 4. Computational investigation into the C–C bond forming mechanism. (A) Potential energy surface of alkynylation via an inner-sphere pathway. (B) Reductive elimination transition state structures reveal favourable non-covalent halogen-π interaction in **TS1$_R$**. (B3LYP-D3(BJ)/def2-TZVP-SMD(toluene)//B3LYP-D3(BJ)/def2-SVP-SMD(toluene)). Alkyl fragment is coloured green. The forming C–C bond is coloured red.

Conclusions

In summary, we have developed a Cu-catalyzed enantioconvergent deborylative alkynylation protocol. This method is compatible with a wide range of functional groups and heterocycles. The alkynylation product can be obtained on a gram scale with a good level of enantiomeric enrichment. Mechanistic evidence suggests the generation of a prochiral radical in a stereoablative fashion, followed by enantioselective radical trapping by a Cu(II) intermediate. DFT calculation supports the viability of an inner-sphere mechanism and attributes the observed enantioselectivity to ligand-substrate halogen-π interactions.

Author contributions

YD conceptualized the work. JFH, YD, and BZ performed the experiments in this project. TJS carried out the computational work. YD, JFH, and TJS prepared the manuscript.

Conflicts of interest

There are no conflicts to declare.

Data availability

All experimental procedures and data related to this study can be found in the ESI.

Acknowledgements

Notes and references

1. Coca, A., *Boron Reagents in Synthesis*. American Chemical Society: 2016.
2. Fyfe, J. W. B.; Watson, A. J. B., Recent Developments in Organoboron Chemistry: Old Dogs, New Tricks. *Chem* **2017**, *3*, 31-55.
3. Fernández, E.; Whiting, A., *Synthesis and Application of Organoboron Compounds*. Springer International Publishing: 2015.
4. Yang, X.; Kalita, S. J.; Maheshuni, S.; Huang, Y.-Y., Recent advances on transition-metal-catalyzed asymmetric tandem reactions with organoboron reagents. *Coord. Chem. Rev.* **2019**, *392*, 35-48.
5. Matteson, D. S., *Stereodirected Synthesis with Organoboranes*. Springer Berlin Heidelberg: 2012.
6. Collins, B. S. L.; Wilson, C. M.; Myers, E. L.; Aggarwal, V. K., Asymmetric Synthesis of Secondary and Tertiary Boronic Esters. *Angew. Chem. Int. Ed.* **2017**, *56*, 11700-11733.
7. Thomas, S. P.; French, R. M.; Jheengut, V.; Aggarwal, V. K., Homologation and alkylation of boronic esters and boranes by 1,2-metallate rearrangement of boron ate complexes. *Chem. Record* **2009**, *9*, 24-39.
8. Lehmann, J. W.; Blair, D. J.; Burke, M. D., Towards the generalized iterative synthesis of small molecules. *Nat. Rev. Chem.* **2018**, *2*, 0115.
9. Wang, H.; Jing, C.; Noble, A.; Aggarwal, V. K., Stereospecific 1,2-Migrations of Boronate Complexes Induced by Electrophiles. *Angew. Chem. Int. Ed.* **2020**, *59*, 16859-16872.
10. Klis, T.; Lulinski, S.; Serwatowski, J., Formation and Synthetic Applications of Metalated Organoboranes. *Curr. Org. Chem.* **2010**, *14*, 2549-2566.
11. Marek, I.; Normant, J.-F., Synthesis and Reactivity of sp^3-Geminated Organodimetallics. *Chem. Rev.* **1996**, *96*, 3241-3268.
12. Hong, K.; Liu, X.; Morken, J. P., Simple Access to Elusive α-Boryl Carbanions and Their Alkylation: An Umpolung Construction for Organic Synthesis. *J. Am. Chem. Soc.* **2014**, *136*, 10581-10584.
13. Nallagonda, R.; Karimov, R. R., Copper-Catalyzed Regio- and Diastereoselective Additions of Boron-Stabilized Carbanions to Heteroarenium Salts: Synthesis of Azaheterocycles Containing Contiguous Stereocenters. *ACS Catal.* **2021**, *11*, 248-254.
14. Lee, B.; Chirik, P. J., Ketone Synthesis from Benzyldiboronates and Esters: Leveraging α-Boryl Carbanions for Carbon–Carbon Bond Formation. *J. Am. Chem. Soc.* **2020**, *142*, 2429-2437.
15. Jin, H.; Han, J.; Liu, X.; Feng, C.; Zhan, M., Access to Diverse Organoborons by α-Deprotonation and Functionalization of Benzylboronates. *Org. Lett.* **2023**, *25*, 4168-4172.
16. Hartwig, J. F., *Organotransition Metal Chemistry: From Bonding to Catalysis*. University Science Books: 2010.
17. Wang, Y.; Noble, A.; Myers, E. L.; Aggarwal, V. K., Enantiospecific Alkynylation of Alkylboronic Esters. *Angew. Chem. Int. Ed.* **2016**, *55*, 4270-4274.
18. Xu, N.; Liang, H.; Morken, J. P., Copper-Catalyzed Stereospecific Transformations of Alkylboronic Esters. *J. Am. Chem. Soc.* **2022**, *144*, 11546-11552.
19. Golden, D. L.; Suh, S.-E.; Stahl, S. S., Radical C(sp^3)–H functionalization and cross-coupling reactions. *Nat. Rev. Chem.* **2022**, *6*, 405-427.
20. Wang, F.; Chen, P.; Liu, G., Copper-Catalyzed Radical Relay for Asymmetric Radical Transformations. *Acc. Chem. Res.* **2018**, *51*, 2036-2046.
21. Zhang, Z.; Chen, P.; Liu, G., Copper-catalyzed radical relay in C(sp^3)–H functionalization. *Chem. Soc. Rev.* **2022**, *51*, 1640-1658.
22. Fu, L.; Zhang, Z.; Chen, P.; Lin, Z.; Liu, G., Enantioselective Copper-Catalyzed Alkynylation of Benzylic C–H Bonds via Radical Relay. *J. Am. Chem. Soc.* **2020**, *142*, 12493-12500.
23. Fu, L.; Zhou, S.; Wan, X.; Chen, P.; Liu, G., Enantioselective Trifluoromethylalkynylation of Alkenes via Copper-Catalyzed Radical Relay. *J. Am. Chem. Soc.* **2018**, *140*, 10965-10969.
24. Xia, H.-D.; Li, Z.-L.; Gu, Q.-S.; Dong, X.-Y.; Fang, J.-H.; Du, X.-Y.; Wang, L.-L.; Liu, X.-Y., Photoinduced Copper-Catalyzed Asymmetric Decarboxylative Alkynylation with Terminal Alkynes. *Angew. Chem. Int. Ed.* **2020**, *59*, 16926-16932.
25. Dong, X.-Y.; Zhang, Y.-F.; Ma, C.-L.; Gu, Q.-S.; Wang, F.-L.; Li, Z.-L.; Jiang, S.-P.; Liu, X.-Y., A general asymmetric copper-catalysed

Sonogashira C(sp³)–C(sp) coupling. *Nature Chem.* **2019**, *11*, 1158-1166.

26. Lei, G.; Zhang, H.; Chen, B.; Xu, M.; Zhang, G., Copper-catalyzed enantioselective arylalkynylation of alkenes. *Chem. Sci.* **2020**, *11*, 1623-1628.

27. Mo, X.; Guo, R.; Zhang, G., Recent Developments in Copper(I)-Catalyzed Enantioselective Alkynylation Reactions via a Radical Process. *Chin. J. Chem.* **2023**, *41*, 481-489.

28. Zhang, Y.; Sun, Y.; Chen, B.; Xu, M.; Li, C.; Zhang, D.; Zhang, G., Copper-Catalyzed Photoinduced Enantioselective Dual Carbofunctionalization of Alkenes. *Org. Lett.* **2020**, *22*, 1490-1494.

29. Dong, X.-Y.; Cheng, J.-T.; Zhang, Y.-F.; Li, Z.-L.; Zhan, T.-Y.; Chen, J.-J.; Wang, F.-L.; Yang, N.-Y.; Ye, L.; Gu, Q.-S.; Liu, X.-Y., Copper-Catalyzed Asymmetric Radical 1,2-Carboalkynylation of Alkenes with Alkyl Halides and Terminal Alkynes. *J. Am. Chem. Soc.* **2020**, *142*, 9501-9509.

30. Li, J.; Ning, L.; Tan, Q.; Feng, X.; Liu, X., Asymmetric Sonogashira C(sp³)–C(sp) bond coupling enabled by a copper(I) complex of a new guanidine-hybrid ligand. *Org. Chem. Front.* **2022**, *9*, 6312-6318.

31. Bakhoda, A.; Okoromoba, O. E.; Greene, C.; Boroujeni, M. R.; Bertke, J. A.; Warren, T. H., Three-Coordinate Copper(II) Alkynyl Complex in C–C Bond Formation: The Sesquicentennial of the Glaser Coupling. *J. Am. Chem. Soc.* **2020**, *142*, 18483-18490.

32. Ollivier, C.; Renaud, P., Organoboranes as a Source of Radicals. *Chem. Rev.* **2001**, *101*, 3415-3434.

33. Renaud, P.; Beauseigneur, A.; Brecht-Forster, A.; Becattini, B.; Darmency, V.; Kandhasamy, S.; Montermini, F.; Ollivier, C.; Panchaud, P.; Pozzi, D.; Scanlan, E. M.; Schaffner, A.-P.; Weber, V., Boron: A key element in radical reactions. *Pure Appl. Chem.* **2007**, *79*, 223-233.

34. Wang, Z.; Wierich, N.; Zhang, J.; Daniliuc, C. G.; Studer, A., Alkyl Radical Generation from Alkylboronic Pinacol Esters through Substitution with Aminyl Radicals. *J. Am. Chem. Soc.* **2023**, *145*, 8770-8775.

35. Vu, J.; Haug, G. C.; Li, Y.; Zhao, B.; Chang, C. J.; Paton, R. S.; Dong, Y., Enantioconvergent Cross-Nucleophile Coupling: Copper-Catalyzed Deborylative Cyanation. *Angew. Chem. Int. Ed.* **2024**, *63*, e202408745.

36. Zhu, C.; Lin, J.; Bao, X.; Wu, J., Development of N-centered radical scavengers that enables photoredox-catalyzed transition-metal-free radical amination of alkyl pinacol boronates. *Nat. Commun.* **2025**, *16*, 3225.

37. Davies, I. W.; Deeth, R. J.; Larsen, R. D.; Reider, P. J., A CLFSE/MM study on the role of ligand bite-angle in Cu(II)-catalyzed Diels-Alder reactions. *Tetrahedron Lett.* **1999**, *40*, 1233-1236.

38. Proctor, R. S. J.; Colgan, A. C.; Phipps, R. J., Exploiting attractive non-covalent interactions for the enantioselective catalysis of reactions involving radical intermediates. *Nature Chem.* **2020**, *12*, 990-1004.

39. Lu, G.; Liu, R. Y.; Yang, Y.; Fang, C.; Lambrecht, D. S.; Buchwald, S. L.; Liu, P., Ligand–Substrate Dispersion Facilitates the Copper-Catalyzed Hydroamination of Unactivated Olefins. *J. Am. Chem. Soc.* **2017**, *139*, 16548-16555.

40. Jiang, S.; Zhang, L.; Cui, D.; Yao, Z.; Gao, B.; Lin, J.; Wei, D., The Important Role of Halogen Bond in Substrate Selectivity of Enzymatic Catalysis. *Sci. Rep.* **2016**, *6*, 34750.

41. Another interpretation of the results involves the deprotonation of meso-hydrogen to generate an anionic BOX ligand. We tested this hypothesis by subjecting a mixture of ligand **L6**, Cu source, and Cs₂CO₃ to reaction conditions. No deprotonation of the ligand **L6** was observed by ¹H NMR spectroscopy.

42. Shah, M. B.; Liu, J.; Zhang, Q.; Stout, C. D.; Halpert, J. R., Halogen–π Interactions in the Cytochrome P450 Active Site: Structural Insights into Human CYP2B6 Substrate Selectivity. *ACS Chem. Biol.* **2017**, *12*, 1204-1210.

43. Jian, J.; Poater, J.; White, P. B.; McKenzie, C. J.; Bickelhaupt, F. M.; Mecinović, J., Probing Halogen–π versus CH–π Interactions in Molecular Balance. *Org. Lett.* **2020**, *22*, 7870-7873.

44. Jampilek, J., Heterocycles in Medicinal Chemistry. *Molecules* **2019**, *24*, 3839.

45. Heravi, M. M.; Zadsirjan, V., Prescribed drugs containing nitrogen heterocycles: an overview. *RSC Adv.* **2020**, *10*, 44247-44311.

46. Taylor, R. D.; MacCoss, M.; Lawson, A. D. G., Rings in Drugs. *J. Med. Chem.* **2014**, *57*, 5845-5859.

47. Rojas, J. J.; Bull, J. A., Oxetanes in Drug Discovery Campaigns. *J. Med. Chem.* **2023**, *66*, 12697-12709.

48. Becke, A. D., Density-functional thermochemistry. III. The role of exact exchange. *J. Chem. Phys.* **1993**, *98*, 5648-5652.

49. Lee, C.; Yang, W.; Parr, R. G., Development of the Colle-Salvetti correlation-energy formula into a functional of the electron density. *Phys. Rev. B* **1988**, *37*, 785-789.

50. Stephens, P. J.; Devlin, F. J.; Chabalowski, C. F.; Frisch, M. J., Ab Initio Calculation of Vibrational Absorption and Circular Dichroism Spectra Using Density Functional Force Fields. *J. Phys. Chem.* **1994**, *98*, 11623-11627.

51. Vosko, S. H.; Wilk, L.; Nusair, M., Accurate spin-dependent electron liquid correlation energies for local spin density calculations: a critical analysis. *Can. J. Phys.* **1980**, *58*, 1200-1211.

52. Weigend, F.; Ahlrichs, R., Balanced basis sets of split valence, triple zeta valence and quadruple zeta valence quality for H to Rn: Design and assessment of accuracy. *Phys. Chem. Chem. Phys.* **2005**, *7*, 3297-3305.

53. Weigend, F., Accurate Coulomb-fitting basis sets for H to Rn. *Phys. Chem. Chem. Phys.* **2006**, *8*, 1057-1065.

54. Neese, F.; Wennmohs, F.; Becker, U.; Riplinger, C., The ORCA quantum chemistry program package. *J. Chem. Phys.* **2020**, *152*.

55. Initial oxidation of Cu(I) alkynyl intermediate with (ᵗBuO)₂ is exergonic (−0.9 kcal/mol), resulting in the formation of divalent complex **8** (Scheme S3).

56. The deviation from linearity weakens the interaction and likely underlies the modest enantioselectivity observed experimentally.

57. Lu, Y.; Wang, Y.; Zhu, W., Nonbonding interactions of organic halogens in biological systems: implications for drug discovery and biomolecular design. *Phys. Chem. Chem. Phys.* **2010**, *12*, 4543-4551.

58. Consistent with our model, low to moderate levels of enantioselectivity were observed in coupling reactions with alkynes bearing electron-deficient arenes and alkyl groups. (Table S3) Although substrate **3o** containing isoquinoline was obtained with good enantioselectivity, the electron-withdrawing aza-group is not incorporated in the arene directly engaging in Br–π attraction.

The data supporting this article have been included as part of the Supplementary Information.

Crystallographic data for **3c** and **3l** has been deposited at the CCDC under 2446256-2446257 and can be obtained from:

https://www.ccdc.cam.ac.uk/structures/Search?access=referee&ccdc=2446257&Author=Yuyang+Dong

https://www.ccdc.cam.ac.uk/structures/Search?access=referee&ccdc=2446256&Author=Yuyang+Dong